Molecular design of liquid crystalline poly(ester-amide)s with perfluoroalkyl spacers

May May Teoh[a]; Tai-Shung Chung Corresponding author[a]; Si-Xue Cheng[b]; Ting Ting Lin[c]; K. P. Pramoda[c]

[a] Department of Chemical and Environmental Engineering, National University of Singapore, Singapore 119260 [b] Department of Chemistry, Wuhan University, Wuhan 430072, PR China [c] Institute of Materials Research and Engineering, Singapore 117602

PLEASE SCROLL DOWN FOR ARTICLE

Molecular design of liquid crystalline poly(ester-amide)s with perfluoroalkyl spacers

MAY MAY TEOH, TAI-SHUNG CHUNG*

Department of Chemical and Environmental Engineering, National University of Singapore, 10 Kent Ridge Crescent, Singapore 119260

SI-XUE CHENG

Department of Chemistry, Wuhan University, Wuhan 430072, PR China

TING TING LIN and K. P. PRAMODA

Institute of Materials Research and Engineering, 3 Research Link, Singapore 117602

We have introduced a series of perfluoroalkyl dicarboxylic acids with different lengths of fluorinated aliphatic segments into the 2,6-acetoxynaphthoic acid (ANA) and acetoxy acetanilide (AAA) systems; and their effects on the evolution of liquid crystal texture and liquid crystallinity have been investigated. The perfluoroalkyl dicarboxylic acids are tetrafluorosuccinic acid (TFSA, $n=2$), hexafluoroglutaric acid (HFGA, $n=3$), perfluoro-suberic acid (PFSUA, $n=6$) and perfluorosebacic acid (PFSEA, $n=8$). Computational results based on the 'RIS' Metropolis Monte Carlo method indicate that the ANA/AAA/ perfluoroalkyl system may form thermotropic liquid crystalline polymers (LCPs) because the calculated persistence ratios are greater than 6.42. Computational results also predict that the systems containing even-numbered perfluoroalkyl acids have greater persistence length and molar stiffness than that containing odd-numbered acids. Experiments were carried out using the *in situ* thin film polymerization technique under a polarizing optical microscope. We observed that systems containing short aliphatic units ($n=2, 3$) tend to remain in the LC phase, while systems containing a long aliphatic spacer ($n=8$) tend to crystallize during the late stage of the polycondensation reaction. The liquid crystal domain formed in the early stage has a disclination strength S of $+1$. Ternary phase diagrams were plotted to show the relationship among monomer structure, composition, anisotropic and crystalline phases. FTIR results confirm the formation of LCPs.

1. Introduction

Main chain thermotropic liquid crystalline polymers (LCPs) were first synthesized in the early 1970s [1–7]. Wholly aromatic liquid crystalline polyesters and polyamides have received most attention because of their unique properties [7–11]. The recent direction of research and development of LCPs is towards the molecular design of main chain LCPs in order to fulfill either functional characteristics or lower material costs. Although many approaches, such as tailoring the molecular structure with swivel structures, kinks, flexible bonds and lateral groups, have been extensively employed [7–16], studies on the relationship between liquid crystalline heterogeneity and the chain rigidity, persistence ratio

and chemical structure, by means of both experiments and computational simulation, are very limited.

The introduction of aliphatic spacers linking mesogenic groups has been one of many well received study subjects. The uses of aliphatic monomers has dramatically reduced T_m and improved chain flexibility [8–16]. Common aliphatic moieties employed are alkyl and alkoxy units, $-(CH_2)_n-$ and $-(OCH_2CH_2)_n-$, with different flexible spacer lengths [11, 17–21]. With respect to wholly aromatic LCPs, those containing a relatively small concentration of the aliphatic have better processability, with improved transverse mechanical properties. Although the addition of aliphatic spacers could dramatically reduce the polymer transition temperatures (T_m and T_g), a serious drawback of this approach is the disturbance of liquid crystallinity.

*Author for correspondence; e-mail: chencts@nus.edu.sg

A growing number of researchers now share an interest in incorporating fluorine units into thermotropic and lyotropic LCPs [22–28]. However, they focus either on (1) fluorinated LCPs with lateral substituents such as CF_3, CF_3O, CHF_2O or F as a ring substitution, or (2) LCPs linked with alternative fluorocarbon-hydrocarbon segments, $-(CH_2)_m-(CF_2)_n-$. Surprisingly, to our best knowledge, there has been no study of LCPs synthesized from wholly perfluoroalkyl aliphatic segments.

A series of aliphatic perfluoroalkyl dicarboxylic acid monomers, such as tetrafluorosuccinic acid (TFSA), hexafluoroglutaric acid (HFGA), perfluorosuberic acid (PFSUA) and perfluorosebacic acid (PFSEA) with $-(CF_2)_n-$ spacers ($n = 2$, 3, 6 and 8) was chosen in this study. Since fluorine is similar to hydrogen in size but induces a larger dipole, the perfluorinated LCPs may possess greater chain rigidity and more stable mesomorphic phases. The purpose of this study is therefore to examine the effects of wholly perfluoroalkyl aliphatic flexible spacers on the persistence ratio and generation of the liquid crystal state. The monomers selected for this study are shown in figure 1. A thin film polymerization technique was employed to investigate the *in situ* polymerization and evolution of LC texture in the 2,6-acetoxynaphthoic acid/acetoxyacetanalide/perfluoro dicarboxylic acid system. The study of heteroaromatic and non-aromatic (aliphatic) monomeric units on LCPs may bring structural novelty to LCPs, lowering T_m without significantly sacrificing liquid crystallinity.

2. Experimental

2.1. *Monomers*

2,6-Acetoxynapthoic acid (ANA) was synthesized by acetylating 2,6-hydroxynaphthoic acid (HNA) with acetic anhydride in the presence of a pyridine catalyst. The monomer, ANA was purified by recrystallization from methanol. Acetoxy acetanilide (AAA) was prepared by the reaction of *p*-aminophenol with acetic anhydride in NaOH solution at a low temperature, then recrystallized from 50/50 methanol/hexane [29]. The melting points for ANA and AAA were 226 and 157°C, respectively, measured by DSC (Perkin-Elmer DSC Pyris 1). TFSA, HFGA, PFSUA and PFSEA were purchased from Aldrich and used as received. The melting points for TFSA, HFGA, PFSUA and PFSEA are 118, 92, 139, and 151°C, respectively.

2.2. *Thin film polymerization*

The first step of sample preparation was the physical mixing of the monomers by grinding them together according to a specific molar ratio to obtain a homogenous mixture. A sample of the monomer mixture was then placed on a microscopy cover slide. One drop of acetone was applied to the slide to dissolve the monomers. After the solvent had evaporated, a thin layer of monomer mixture remained coated on the glass slide. The thickness of the specimens was within 5–10 μm. The thin film was sandwiched between two glass slides with a 0.5-mm stainless steel spacer ring, while the reactants were placed on the top. The ring spacer provided space for the removal or release of acetic acid during polymerization. Without the spacer, it was found that reproducibility was quite low and the film quality was poor because the evaporation (or release) of acetic acid at elevated temperatures was vigorous.

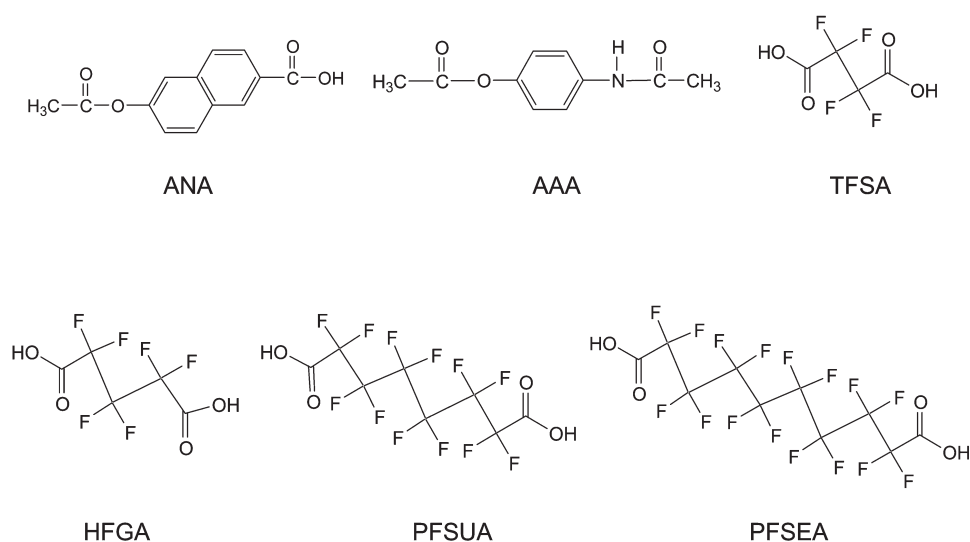The specimen was then placed on the hot stage (Linkam THMS-600) of a polarizing optical

Figure 1. Chemical structure of the monomers.

microscope (Olympus BX50). The temperature was raised at 90°C min^{-1} to a desired level and time measurement was started at this temperature. During the *in situ* polymerization, images of morphological changes were recorded and analysed by an imaging software (Image-Pro Plus 3.0). A detailed description of experimental procedures for *in situ* thin film polymerization has been published elsewhere [28–32].

2.3. *Fourier transform infrared spectroscopy characterization*

The monomers and polymers (in KBr pellets) were characterized by FTIR (Perkin-Elmer FTIR Spectrometer Spectrum 2000) with a wave number range of 4000–400 cm^{-1} and a resolution of 4 cm^{-1}.

2.4. *RMMC (the 'RIS' Metropolis Monte Carlo method), Cerius^2 computational simulation*

A RMMC (the 'RIS' Metropolis Monte Carlo method) module within the Cerius^2 software package was used to calculate the properties of polymer chains, such as the mean squared end-to-end distance, mean squared radius of gyration, persistence length and molar stiffness function of the monomers and polymer chains. A Chem-3D Pro software was employed to determine the diameter of polymer chains (5.5 Å) for the estimation of persistence ratios.

3. Results and discussion
#### 3.1. *Computational simulation*

Table 1 summarizes the calculated results of polymer chain properties for the ANA/AAA/perfluoroalkyl system. The molar ratio in the simulation was 5:1:1 with 20 repeated units. The following observations can

be made: (1) molecules with a longer perfluoroalkyl chain usually have a higher mean squared end-to-end distance, mean squared radius of gyration, persistence length, and persistence ratio; (2) the even-numbered series have a more rigid-rod backbone and a higher level of chain stiffness than the odd-numbered series; (3) the molar stiffness increases linearly with an increase in the number of perfluoroalkyl repeat units; (4) the odd-numbered unit ($n = 3$) yields LCPs having the lowest stiffness and persistence length among the four perfluoroalkyl systems studied.

As predicted by Flory and Ronca [33], the critical aspect ratio of the rod molecules for thermotropic liquid crystallinity is 6.42. In our study, the persistence ratios for the ANA/AAA/perfluoroalkyl system with $n = 2$, 3, 6, and 8 were 6.50, 6.47, 7.16 and 8.10, respectively. Thus, the simulation results clearly support the possibility of thermotropic LCP formation. According to the continuum theory of LCs, the higher the elastic constant is, the larger the distortion energy. Based on the Odijk presumption, the splay, twist, and bend elastic constants increase with an increase in persistence length or persistence length/diameter (persistence ratio, q/d) [34, 35]. Therefore, the ANA/AAA/perfluoroalkyl system having even or higher n may exhibit strong LC characteristics. In addition, the calculated mean squared end-to-end distance and mean squared radius of gyration increase significantly with increasing number of –CF$_2$– repeated units, indicating that (1) the polymer chains form a worm-like structure with the spacer linkage in the rigid-rod backbone, or (2) the excess electronegative fluorine charge results in an increase in the free volume among polymer chains.

Table 2 compares the calculated persistence length, persistence ratio and molar stiffness for polymers made

Table 1. The properties of polymer chains with different flexible linkages (20 repeated units) at 280°C, simulated by RMMC – Cerius^2 Molecular Simulation Software.
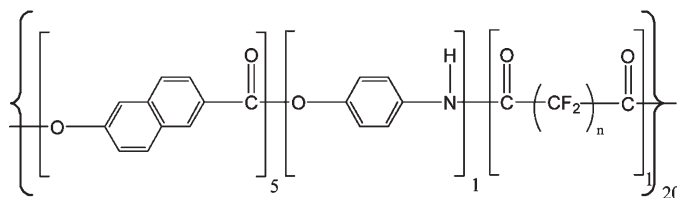
Properties of polymer chains	TFSA ($n=2$)	HFGA ($n=3$)	PFSUA ($n=6$)	PFSEA ($n=8$)
Mean squared end-to-end distance/Å^2	30 809	28 265	47 434	68 350
Mean squared radius of gyration/Å^2	4947	4691.7	7782	10 639
Persistence length/Å	35.75	35.61	39.40	44.54
Persistence ratio	6.50	6.47	7.16	8.10
Molar stiffness function/g$^{0.25}$cm$^{1.5}$/mol$^{0.75}$	100.5	96.17	126.4	195.8

Table 2. The properties of polymer chains with different lengths of flexible linkage on methyl and perfluoroalkyl (20 repeat units), P(ONA) (100 repeat units) and Vectra B (20 repeated units) at 280°C, simulated by RMMC – Cerius^2 Molecular Simulation Software.

Properties of polymer chains

$(X)_n$	$(CH_2)_3$	$(CF_2)_3$	$(CH_2)_8$	$(CF_2)_8$		
Mean squared end-to-end distance/Å^2	30 954	28 265	41 128	68 350	61 035	14 180
Mean squared radius of gyration/Å^2	5053.5	4691.7	6714.1	10 639	9577	19 390
Persistence length/Å	35.01	35.61	36.43	44.54	41.19	112.09
Persistence ratio	6.37	6.47	6.6	8.10	7.49	20.38
Molar stiffness function/ g$^{0.25}$cm$^{1.5}$/mol$^{0.75}$	100.5	96.17	126.4	195.8	168.5	417.3

from a hypothetical molar ratio of 5:1:1 with 20 repeated units of ANA/AAA/alkyl, ANA/AAA/ perfluoroalkyl, as well as a commercial LCP, ANA/ AAA/TA (Vectra^{TM} B), and a wholly aromatic poly(2,6-oxynaphthoate) (PONA) with 100 repeated units. Compared with Vectra B, the addition of alkyl and perfluoroalkyl spacers with $n = 3$ significantly reduces the stability and rigidity of the mesogenic structure. However, the reduction in persistence ratio and molar stiffness becomes smaller when LCPs are synthesized from even-numbered perfluoroalkyl groups with a high number of –CF$_2$– units. Remarkably, the persistence ratio and molar stiffness of the ANA/AAA/PFSEA ($n = 8$) system are higher than those of Vectra B and are the highest among the systems studied. These features energetically favour the formation of liquid crystal or crystal structure.

The fluorine atom has a much higher atomic weight, but only 10% larger van der Waals radius than hydrogen. Thus the packing density of the fluorocarbon segment exceeds by far that of the hydrocarbon segment. For systems made from three repeated units of –CH$_2$– and –CF$_2$–, there is little difference between them in terms of persistence length and molar stiffness. However, for eight repeated units, the incorporation of fluorine into the system radically increases the molar stiffness by 35%, and the persistence length by 18%. This may arise from two possible causes: (1) the long perfluorocarboxyl chains have a tendency to adapt a helical conformation [26, 27], and (2) the disparity in cross-section area between hydrocarbon and perfluoro-carbon chains (18.5 vs. 28.3 Å^2) [26, 27].

3.2. *Evolution of LC formation and texture*

Figures 2, 3, and 4 show the evolution of LC texture and microstructure changes during the polymerization of the ANA/AAA/TFSA ($n = 2$) ANA/AAA/HFGA ($n = 3$) and ANA/AAA/PFSUA ($n = 6$) systems at different reaction times. All the micrographs were obtained from the same area of the same sample under a polarizing optical microscope at 280°C for 2 h. The reactions started from monomer mixtures in the crystal phase. Heat was applied and the monomers were melted to the isotropic phase. The change of morphologies follows these sequences: firstly, generation of LC droplets; then coalescence of the LC droplets; then formation of schlieren texture and lastly annihilation of disclinations. Traditionally, thin film polymerizations usually end with either the formation of stripe texture or crystallization [29–32]. However, only crystal and liquid crystal texture are observed for the systems studied.

For the ANA/AAA/TFSA ($n = 2$) system, oligomers are formed in the molten monomer phase in the early stages, and LC droplets start to appear and separate from the isotropic phase once the minimum requirement of persistence ratio for liquid crystallinity is reached. The brighter phase shown in the figures represents the LC phase and the darker view is of the isotropic melt. Molecular mass and LC chain length increase rapidly with time in the early stages (140–220 s), thus the LC phase generation and coalescence of the LC phase take place simultaneously. The overall view area becomes an anisotropic phase (i.e. schlieren texture) at 240 s. After 4 min, no further morphological changes can be seen. Similar patterns of LC texture evolution and micro-structure changes can be observed in figures 3 and 4 for
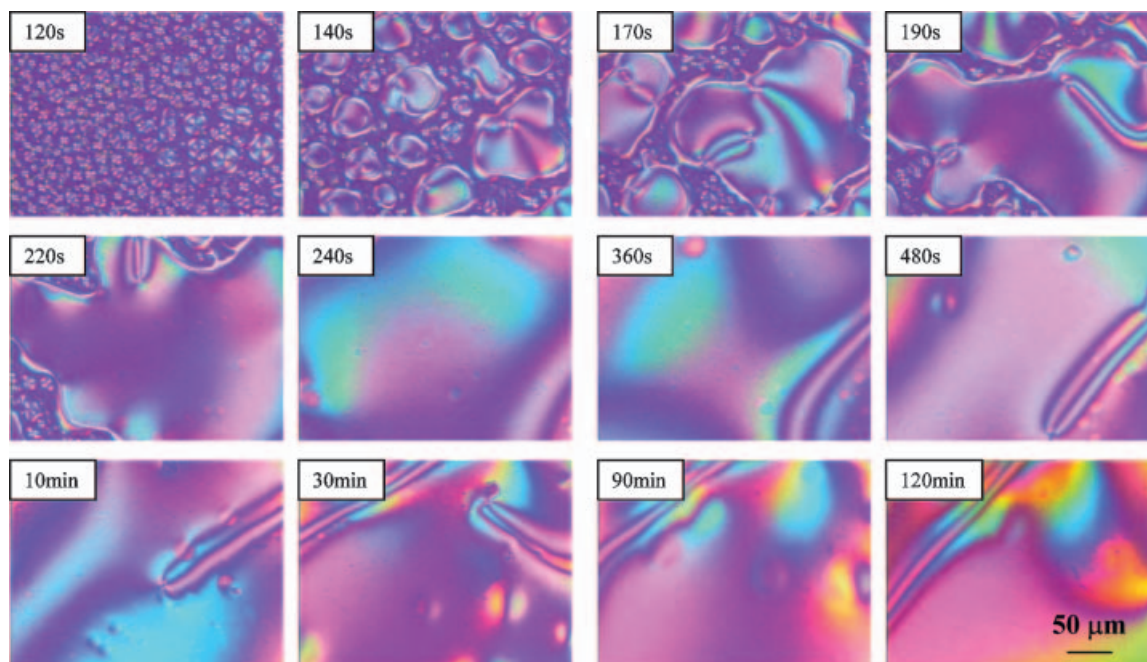
Figure 2. Micrographs showing morphologies of the 70/15/15 ANA/AAA/TFSA polymerization reaction system at different reaction times. All the micrographs were obtained from the same area of the same sample. Reaction temperature: 280°C.
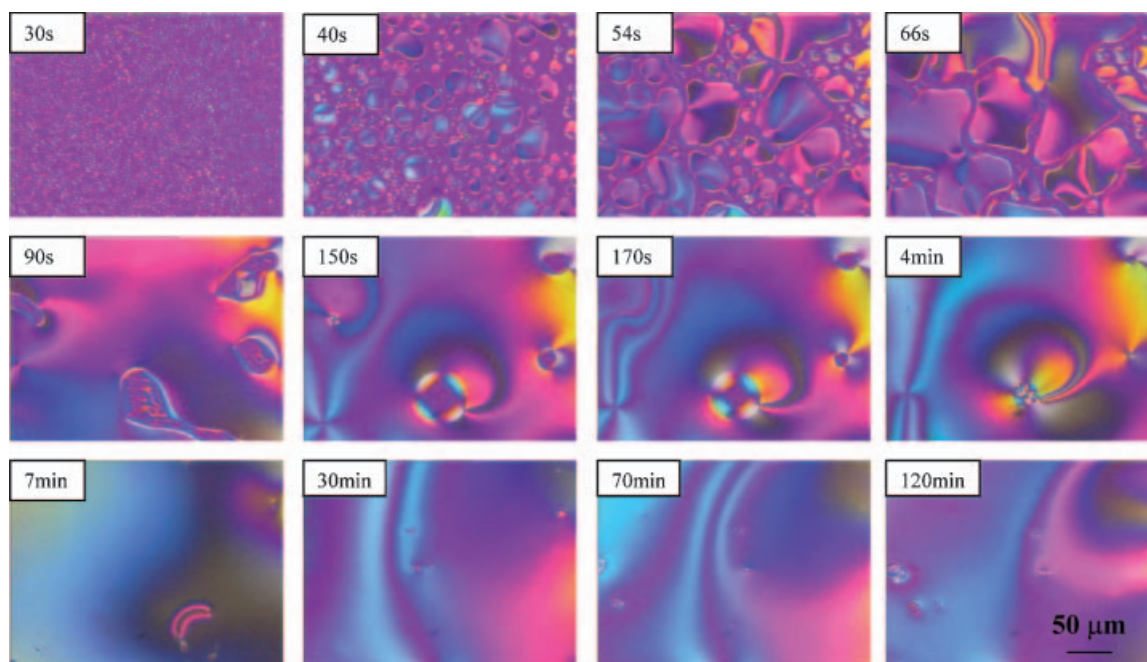

Figure 3. Micrographs showing morphologies of the 70/15/15 ANA/AAA/HFGA polymerization reaction system at different reaction times. All the micrographs were obtained from the same area of the same sample. Reaction temperature: 280°C.

the ANA/AAA/HFGA ($n=3$) and ANA/AAA/PFSUA ($n=6$) systems, respectively. The morphological changes for these systems are quite comparable.

The ANA/AAA/PFSEA ($n=8$) system, with the longest perfluoroalkyl moiety, favours crystallization in the last stages, as illustrated in figure 5. For example,
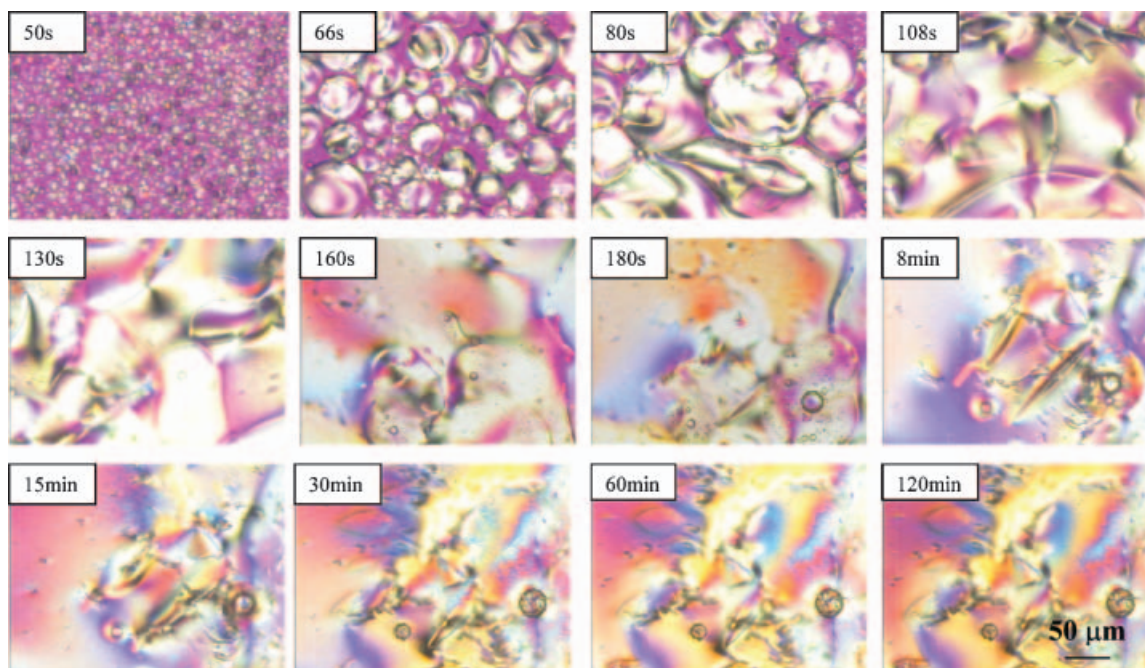
Figure 4. Micrographs showing morphologies of the 70/15/15 ANA/AAA/PFSUA polymerization reaction system at different reaction times. All the micrographs were obtained from the same area of the same sample. Reaction temperature: 280°C.
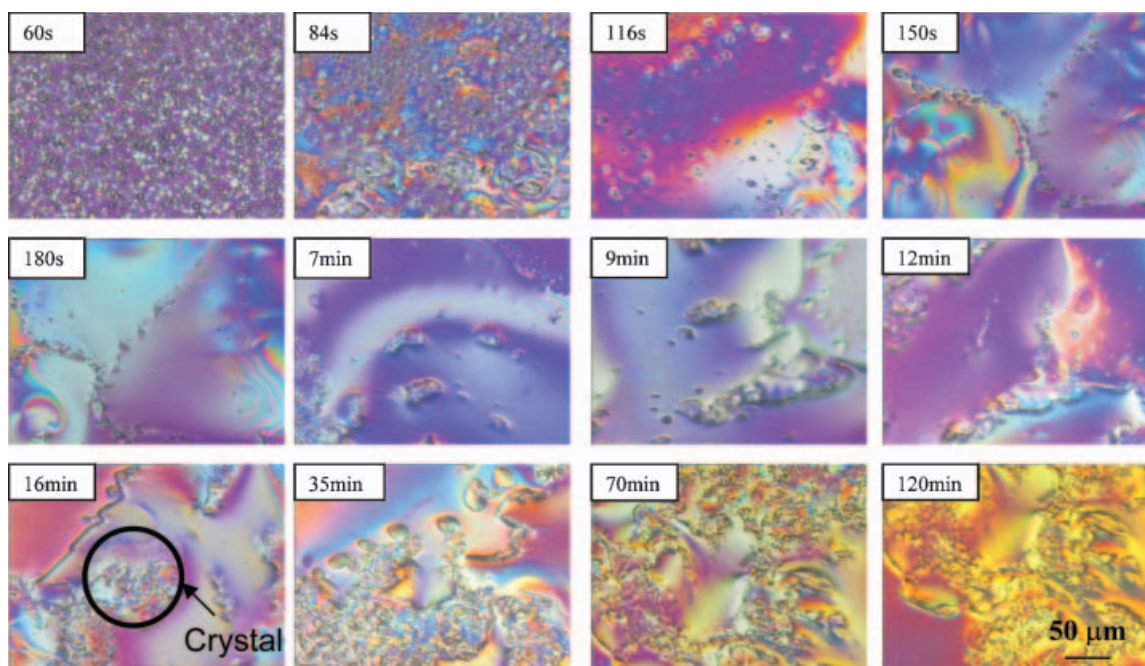

Figure 5. Micrographs showing morphologies of the 70/15/15 ANA/AAA/PFSEA polymerization reaction system at different reaction times. All the micrographs were obtained from the same area of the same sample. Reaction temperature: 280°C.

at 16 min of polymerization, the crystal phase can be clearly discerned (left bottom of figure 5), which is consistent with the computational results. Previous studies suggest that polymers with short repeating units and high symmetry tend to crystallize better than those with long repeating units and low symmetry [26, 32,

36]. In contrast to the earlier studies, we have observed that the longer the repeating unit is, the greater the crystallization. Additionally, the ANA/AAA/HFGA, ANA/AAA/TFSA, and ANA/AAA/PFSUA systems with a shorter aliphatic spacer ($n=3$, 2 and 6) have a more stable LC mesophase than the system with the longest perfluoroalkyl aliphatic spacer ($n=8$).

The perfluoroalkyl aliphatic length has a great effect on the end-stage morphology. Only crystal texture has been observed in the longest perfluoroalkyl linkages, i.e. PFSEA ($n=8$). Yet, for TFSA ($n=2$) HFGA ($n=3$) and PFSUA ($n=6$), the morphological changes stop at the scheliren texture although the reaction was kept maintained for 2 h. The initial time for the appearance of the LC phase is also dependent on the perfluoroalkyl aliphatic substituents. Consistent with the molecular modelling, the ANA/AAA/TFSA ($n=2$) system requires the longest time for the generation of an anisotropic phase because it has low persistence ratio and chain stiffness (as shown in table 1). The ANA/AAA/HFGA system has the lowest persistence ratio and chain stiffness, but forms the LC phase faster than the ANA/AAA/TFSA ($n=2$) system because it has an odd-number perfluoroalkyl chain. Many reports indicate that the liquid crystallinity of LCPs is strongly influenced by the even–odd effect of flexible spacers, which is attributed to the *trans*- and *gauche*-formation [7–9, 11, 12, 19]. As expected, the ANA/AAA/PFSUA ($n=6$) and ANA/AAA/PFSEA ($n=8$) systems have much shorter initial times before the appearance of an LC phase.

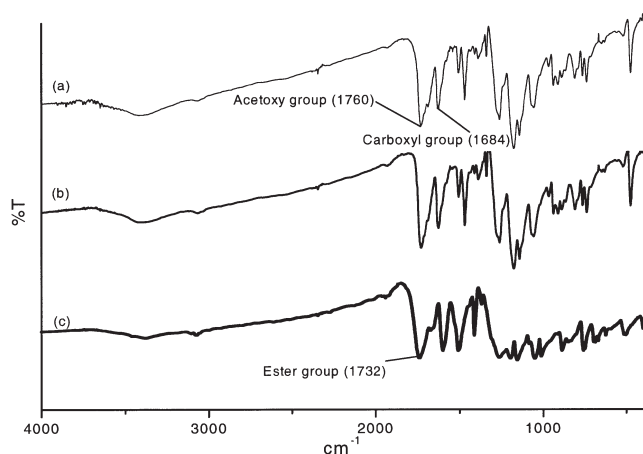The strength S of a disclination during the polymerization was characterized; it was calculated as $|S| = N/4$, where N is the number of dark brushes around a single disclination. To conduct this experiment, we rotated the crossed polarizer and observed the rotated direction of the brushes. If the direction of the rotation is the same as the polarizer, the disclination is positive; the reverse is true for a negative disclination. A disclination strength of $+1$ was observed for the four systems studied, indicating that the dynamics of defect annihilation during the early stage of polymerization may be the same.

3.3. *FTIR characterization*

The FTIR spectra of monomers and copoly(ester-amide)s for the 70/15/15 ANA/AAA/HFGA system were characterized as a function of reaction time and are shown in figure 6. The band at $1760\,cm^{-1}$ represents $v_{c=o}$ of CH_3COO– while the band $1684\,cm^{-1}$ represents $v_{c=o}$ of –COOH. The acetoxy group disappeared entirely with the formation of the ester group band at $1732\,cm^{-1}$, when the polycondensation reaction was maintained at 280°C for 2 h.

3.4. *Critical ANA content for LC formation*

The critical (or minimum) ANA content for formation of the LC phase was determined, as shown in figure 7, for the ANA/AAA/TFSA ($n=2$), ANA/AAA/HFGA ($n=3$) and ANA/AAA/PFSEA ($n=8$) systems. The ANA/AAA/HFGA system requires the lowest temperature for LCP texture formation; at 260°C, 20 mol% ANA is required in this system. Below this critical content, only isotropic or crystal phases are found. Above the critical content, the higher the ANA critical content, the higher the annihilation rates. Below the critical content, the morphology is controlled by crystallization and the rate of crystal growth decreases with increasing ANA content.

In addition, a higher reaction temperature results in a lower critical content. This is possibly because of the rapid increase in molecular weight and persistence ratio at high temperatures. As a consequence, for the same composition a higher reaction temperature usually leads to easier and faster formation of the LC phase. The ANA/AAA/HFGA ($n=3$) system has a higher tendency to yield the LC phase than the ANA/AAA/TFSA ($n=2$) and ANA/AAA/PFSEA ($n=8$) systems, possibly because HFGA has the lowest melting point and possesses an odd-number perfluoroalkyl group. TFSA has a melting point (118°C) between HFGA (92°C) and PFSEA (151°C), thus the critical content of ANA in ANA/AAA/TFSA ($n=2$) is between the other two. The other cause is that the short perfluoroalkyl segments ($n=2$ and 3) in the backbone generally lead to the formation of more stable nematic phases. The zigzag phenomenon on LC formation for the current

Figure 6. The FTIR spectra of 70/15/15 ANA/AAA/HFGA reaction system at 280°C for different reaction times: (*a*) 0 min, (*b*) 1 h, (*c*) 2 h.
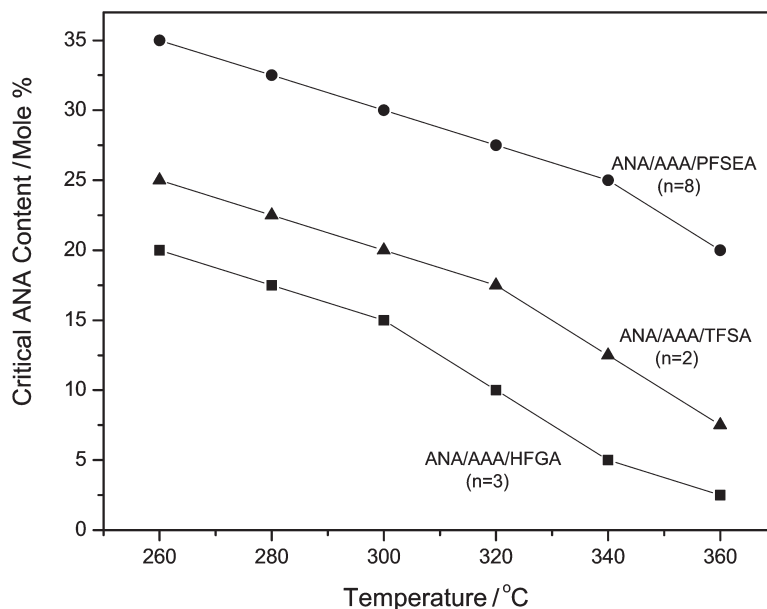
Figure 7. Dependence of the critical ANA content on the reaction temperature.

perfluoroalkyl system appears to be similar to that seen in studies involving the *n*-alkyl system.

The phase diagrams of the ANA/AAA/HFGA (*n* = 3) system and representations of morphologies at 30/60/10 (i.e. AAA rich), 30/35/35, and 30/10/60 (i.e. AAA poor) compositions are shown in figures 8 and 9, respectively. Figures 10 and 11 show the case of the ANA/AAA/ PFSEA (*n* = 8) system and its morphologies at 40/50/10 (i.e. AAA rich), 40/30/30 and 40/10/50 (i.e. AAA poor) compositions. Because the critical molar compositions for LC formation in ANA/AAA, ANA/HFGA and ANA/PFSEA copoly(ester-amide)s are 5/95, 25/75, and 35/65, respectively, any composition in the grey areas in figures 8 and 10 would form an LC phase if the reaction time is 1 h at 300°C. Outside the grey areas and below these critical lines, the LC phase cannot form during the polycondensation reaction. This indicates that, lower ANA content cannot meet the minimum persistence ratio requirement for LC formation. Because the region close to the ANA–AAA axis has more grey areas than the region near the ANA–HFGA (or PFSEA) axis, AAA shows a higher tendency to form LC characteristics than does HFGA (or PFSEA). Although the grey area exhibits LC characteristics, only equal mole percentages of AAA and HFGA (or PFSEA) in an ANA system can lead to high molecular mass LC copoly(ester-amide)s. Polycondensation reactions are deficient if either the AAA or HFGA (PFSEA) content is excessive.

When comparing the evolution of morphology at compositions (a), (b) and (c), figures 9 and 11 show that

AAA plays an important role not only on the reaction time needed for the appearance of a LC phase, but also on the final morphology. It takes 15 min to form LC droplets in the 30/60/10 ANA/AAA/HFGA composition, figure 9 (*a*), but only around 2 min for the 30/35/35, figure 9 (*b*) and 30/10/60 ANA/AAA/HFGA, Figure 9 (*c*) systems. The difference in time needed for LC appearance may arise from different reactivities. The acetoxy group attached to the –NH– (amine) functional group in AAA may lower the reaction rate. A similar phenomenon is also observed for the ANA/ AAA/PFSEA system, as shown in figure 11. In addition, figure 9 shows that AAA content significantly affects morphology. When the AAA content is in the medium to high range (i.e. 35–60%), a stable LC phase is formed. Conversely, a crystal structure is formed if the AAA content is low. If the AAA content is 10%, figure 9 (*c*) indicates that LC droplets start to appear at 100 s, but crystallization takes place rapidly. A similar trend is observed in the ANA/AAA/PFSEA (*n* = 8) system.

4. Conclusions

(1) Novel LCPs made from fluorinated poly(ester-amide)s have been identified; supported by molecular simulation and confirmed by thin film polymerization. Based on computational results, all the systems satisfy the minimum requirement for LC formation with persistence ratios larger than 6.42. Moreover, the results obtained also suggest that the even-numbered
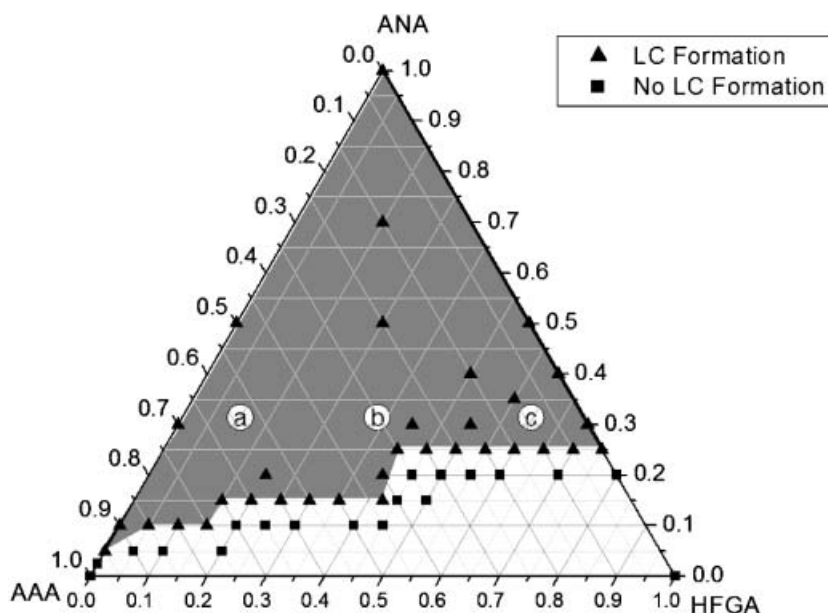
Figure 8. The critical ANA content for LC formation in the ANA/AAA/HFGA system. The reaction temperature was 300°C and reaction compositions were: (*a*) 30/60/10, (*b*) 30/35/35, (*c*) 30/10/60.
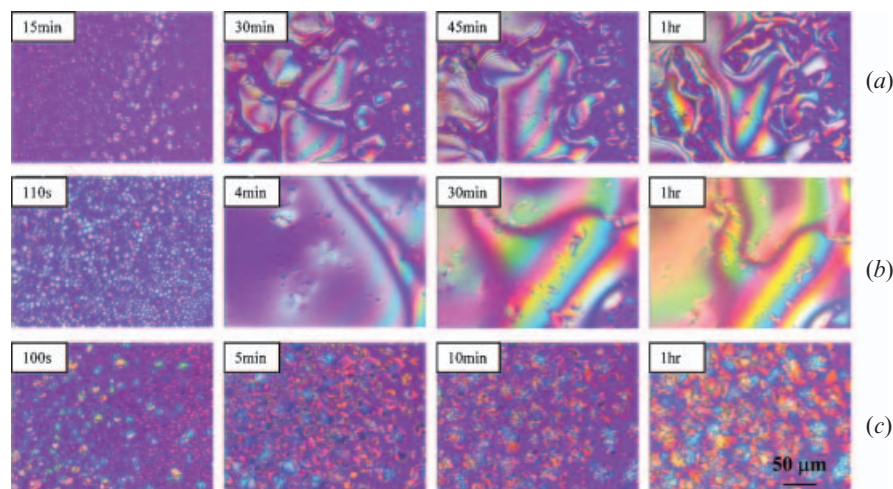

Figure 9. Micrographs showing morphologies of the ANA/AAA/HFGA polymerization reaction system at different reaction compositions: (*a*) 30/60/10, (*b*) 30/35/35, (*c*) 30/10/60. All the micrographs were obtained from the same area of the same sample. Reaction temperature: 300°C.

series have a higher level of chain stiffness and persistence length than the odd-numbered series.

(2) The effects of perfluoroalkyl aliphatic spacers on the LC texture evolution, generation and annihilation have been determined by *in situ* polymerization under a polarizing optical microscope. The longest aliphatic perfluoroalkyl spacer ($n=8$) tends to induce a crystal phase, whereas short aliphatic spacers ($n=2$ and 3) appear to be more favourable for LC formation. The LC

domains formed at the early stage of these aromatic/aliphatic poly(ester-amide)s have a disclination strength of $+1$.

(3) Through ternary monomer phase diagrams, we observed that monomer structure and composition have a great effect on the end stage morphological changes. AAA has a relatively higher tendency to form LC characteristics than HFGA (or PFSEA). Only equimolar AAA and perfluoroalkyl can form high molecular mass
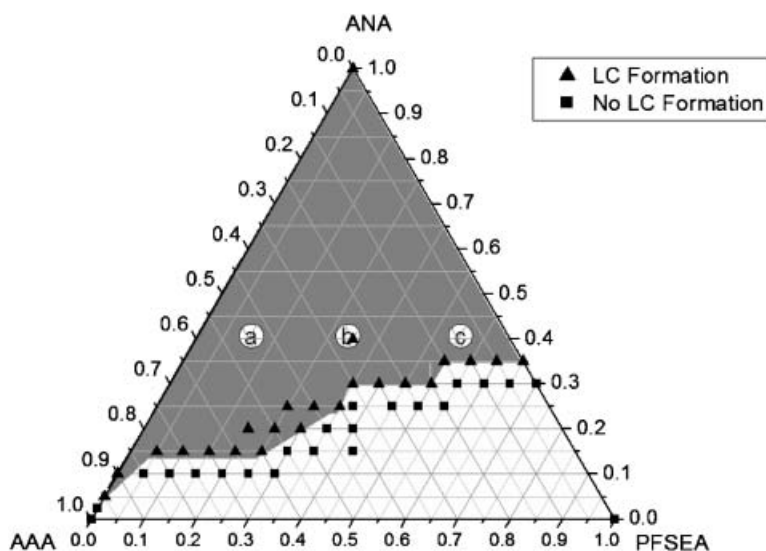
M. M. Teoh *et al.*

Figure 10. The critical ANA content for LC formation in the ANA/AAA/PFSEA system. The reaction temperature was 300°C and reaction compositions were: (*a*) 40/50/10, (*b*) 40/30/30, (*c*) 40/10/50.
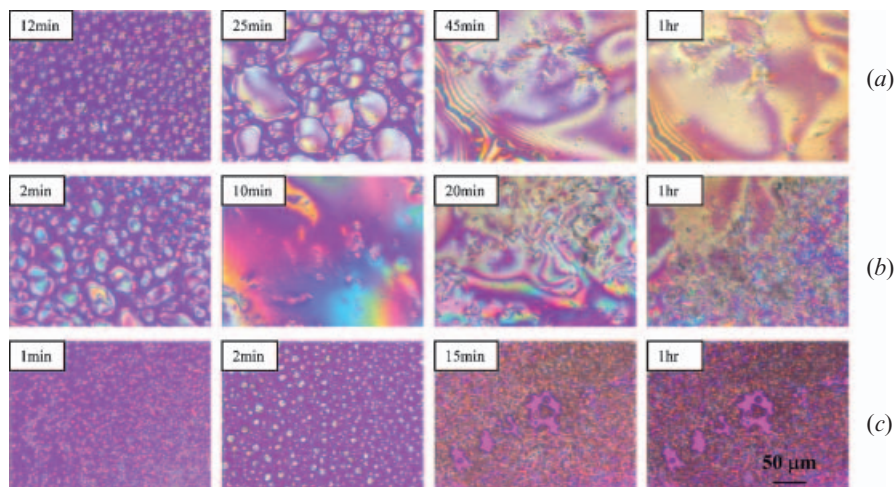

Figure 11. Micrographs showing morphologies of the ANA/AAA/PFSEA polymerization reaction system at different reaction compositions: (*a*) 40/50/10, (*b*) 40/30/30, (*c*) 40/10/50. All the micrographs were obtained from the same area of the same sample. Reaction temperature: 300°C.

LCPs. In addition, FTIR spectra indicate that the acetoxy group completely disappears after the reaction and ester group forms at the end of the reaction.

References

[1] CALUNDANN, G. W., and JAFFE, M., 1982, *Anisotropic Polymers, their Synthesis and Properties*, in Proceedings of the Robert A. Welch Conferences on Chemical Research, XXVI., Synthetic Polymers, p. 247.
[2] COTTIS, S. G., ECONOMY, J., and NOWAK, B. E., 1972, U.S. Patent 3 637 595.
[3] COTTIS, S. G., ECONOMY, J., and NOWAK, B. E., 1976, U.S. Patent 3 975 487.
[4] KUHFUSS, H. F., and JACKSON, W. J., JR, 1973, U.S. Patent 3 778 410.
[5] JACKSON, W. J., JR, and KUHFUSS, H. F., 1976, *J. polym. Chem. Ed.*, **14,** 2043.
[6] PLATE, N. A., and SHIBAEV, V. P., 1984, *Macromol. Chem. Suppl.*, **6,** 3.

[7] CHUNG, T. S., 1986, *Polym. eng. Sci.*, **26**, 901.

[8] WEISS, R. A., and OBER, C. K., 1990, *Liquid Crystalline Polymers* (Washington DC: American Chemical Society).

[9] COLLYER, A. A., 1992, *Liquid Crystal Polymers: From Structure to Application* (London: Elsevier Applied Science).

[10] MANTIA, F. P. L., and MAGAGNINI, P. L., 1997, *Liquid Crystalline Polymers: Handbook of Thermoplastic*, edited by O. Olabisi (New York: Marcel Dekker).

[11] CHUNG, T. S. CHUNG, 2001, *Thermotropic Liquid Crystal Polymers – Thin-Film Polymerization, Characterization, Blend and Application* (New York: CRC press).

[12] COLLYER, A. A., 1989, *Mater. Sci. Tech.*, **5**, 309.

[13] STEGEMEYER, H., 1994, *Liquid Crystals* (New York: Springer).

[14] JIN, J. I., and KANG, C. S., 1997, *Prog. polym. Sci.*, **22,** 937.

[15] CHIELLINI, E., GIORDANO, M., and LEPORINI, D., 1997, *Structure and Transport Properties in Organized Polymeric Material* (Singapore: World Scientific).

[16] PLATE, N. A., 1993, *Liquid Crystal Polymers* (New York and London: Plenum Press).

[17] SHI, F. F., and ECONOMY, J., 1997, *Polym. eng. Sci.*, **37,** 549.

[18] TOMOHITO, H., MORIYUKI, S., and KEN-ICHI, M., 1993, *Macromol. Chem.*, **194,** 2861.

[19] INOUE, T., KAKIMOTO, M., IMAI, Y., and WATANABE, J., 1997, *Macromol. Chem. Phys.*, **198,** 519.

[20] BHOWMIK, P. K., WANG, X. B., and HAN, H. S., 2003, *J. polym. Sci. polym. Chem.*, **41,** 1282.

[21] TOSHIO, I., AKIRA, T., SHINJI, W., MASA-AKI, K. and TOSHIKAZU, K., 2001, *Macromol. Chem. Phys.*, **202,** 26.

[22] BRACON, F., GUITTARD, F., GIVENCHY, E. T., and GERIBALDI, S., 2000, *Polymer*, **41,** 7905.

[23] XIANG, M. L., LI, X. F., OBER, C. K., CHAR, K., GENZER, J., SIVANIAH, E., KRAMER, E. J., and FISCHER, D. A., 2000, *Macromolecules*, **33,** 6106.

[24] BROSTON, W., 1998, *Mechanical and Thermophysical Properties of Polymer Liquid Crystals* (London: Chapman & Hall).

[25] HIYAMA, T., 2000, *Organofluorine Compounds: Chemistry and Application* (New York: Springer).

[26] HOPKEN, J., and MOLLER, M., 1992, *Macromolecules*, **25,** 2482.

[27] VILALTA, P. M., HAMMOND, G. S., and WEISS, R. G., 1993, *Langmuir*, **9,** 1910.

[28] CHENG, S. X., and CHUNG, T. S., 2002, *Polymer*, **43,** 7433.

[29] CHENG, S. X., CHUNG, T. S., and MULLICKOF, S., 1999, *Chem. Eng. Sci.*, **54,** 663.

[30] CHENG, S. X., and CHUNG, T. S., 1999, *J. phys. Chem. B*, **103,** 4923.

[31] CHENG, S. X., and CHUNG, T. S., 2002, *Macromol. Chem. Phys.*, **203,** 122.

[32] CHENG, S. X., CHUNG, T. S., and MULLICKOF, S., 1999, *J. polym. Sci. polym. Phys.*, **37,** 3084.

[33] FLORY, P. J., and RONCA, G., 1979, *Mol. Cryst. liq. Cryst.*, **54,** 311.

[34] WINDLE, A. H., 1994, in *Liquid Crystalline and Mesomorphic Polymers*, edited by V. P. Shibaev and L. Lam (New York: Springer).

[35] CHUNG, T. S., CALUNDANN, G. W., and EAST, A. J., 1989, *Liquid Crystalline Polymers and Their Application: Encyclopedia of Engineering Materials*, Vol. 2 (New York: Marcel Dekker), p. 625.

[36] WUNDERLICH, B., 1973, *Macromolecular Physics – Crystal Nucleation, Growth, Annealing*, Vol. 2 (New York: Academic Press).